

Electrochemical Behavior of Fluorinated and Aminated Nanodiamond

Yanhui Wang, Hao Huang, Jianbing Zang*, Fanwei Meng, Liang Dong, Jing Su

State Key Laboratory of Metastable Material Science & Technology, College of Material Science & Engineering, Yanshan University, Qinhuangdao, P.R. China, 066004

*E-mail: diamondzjb@163.com

Received: 6 July 2012 / Accepted: 20 July 2012 / Published: 1 August 2012

Nanodiamond (ND) powder was fluorinated through direct interaction of elemental fluorine with diamond surfaces and then aminated by chemical substitution reactions using the fluorinated-ND as an intermediate. The effects of the surface terminations on electrochemical properties of ND electrodes were investigated in aqueous solutions containing $\text{Fe}(\text{CN})_6^{3-}/\text{Fe}(\text{CN})_6^{4-}$ and $\text{Fe}^{3+}/\text{Fe}^{2+}$ redox couples. The results showed that both redox reactions of $\text{Fe}(\text{CN})_6^{3-}/\text{Fe}(\text{CN})_6^{4-}$ and $\text{Fe}^{3+}/\text{Fe}^{2+}$ were quasi-reversible on the pristine ND/solution interfaces. The redox kinetics of the $\text{Fe}(\text{CN})_6^{3-}/\text{Fe}(\text{CN})_6^{4-}$ and $\text{Fe}^{3+}/\text{Fe}^{2+}$ systems became slower after fluorination on ND surface. The followed amino modification accelerated the electron exchange between the electrode and $\text{Fe}(\text{CN})_6^{3-}/\text{Fe}(\text{CN})_6^{4-}$ but slowed the redox reaction of $\text{Fe}^{3+}/\text{Fe}^{2+}$ cations. The electrochemical activity of ND powder can be tunable via surface functionalizations.

Keywords: nanodiamond; fluorinate; aminate; surface termination; electrochemical.

1. INTRODUCTION

There is an increasing interest in detonation nanodiamond (ND) because of its unique properties originating from the lattice structure and the large functionalized surface [1, 2]. Surface functional groups absorbed on ND surfaces in detonation synthesis and purification can be varied via chemical pretreatments and thermal annealing for different engineering applications [1, 3, 4]. Those features render it to be interested in numerous technological fields ranging from the use as tribological coatings to bio-interfaces. The creation of specific surface sites on ND for selective molecular attachments is considered a promising approach for their applications in nanofabrication, bioprobes, nanosensors, drug delivery, etc. [5-8].

Recently, increasing interest has arisen in fluorinated ND (F-ND) owing to its attractive properties, for example, high hydrophobicity of the surface, low dielectric constant, and improved tribological properties [9-11]. Especially, F-ND can easily be further modified by chemical substitution reactions and specific functional groups can be bound to the surface (alkyl-, amino-, and amino acid-ND derivatives), thus expanding ND engineering and biomedical applications [9]. Amine-termination of diamond surfaces was also investigated for biomolecule immobilization because of its high nucleophilicity [12]. Amino groups were introduced onto diamond surfaces through various methods for subsequently functionalizing with biomolecules [12-16].

Most recently detonation synthesized nanodiamond (ND) powders have been incorporated into electrodes and biosensors [8, 17-22]. The electrochemical activity is thought to be closely linked to the surface states of ND [23]. In this study, F-ND was prepared through direct interaction of elemental fluorine with diamond surfaces and aminated ND (A-ND) was obtained using F-ND as an intermediate by chemical substitution reactions. The effects of the surface terminations on the electrochemical properties of ND electrodes were investigated.

2. EXPERIMENTAL

2.1 Preparation of F-ND and A-ND

ND powders with average particle size of 5nm synthesized by detonation were supplied by Element Six Ltd. Fluorination treatment was performed in a vacuum chamber with an outer electric furnace. ND powders were put into a stainless vessel and then set in the chamber. After evacuation, fluorine gas was introduced to the chamber at the fluorine pressure of 3.4 kPa, and then the chamber was heated to 350 °C. After fluorinating for 24 h, the sample was cooled to room temperature, and the fluorine was purged with argon. To prepare A-ND, 0.5 g of F-ND was uniformly mixed in 200 mL of ethylenediamine solution in a flask and then the mixture was refluxed at 116 °C for 48 h. After cooling, the mixture was filtrated and washed with deionized water repeatedly.

2.2 Characterizations of F-ND and A-ND

The methods of fourier transform infrared (FTIR) spectra, Raman spectra, and transmission electron microscopy (TEM) were used to characterize the prepared F-ND and A-ND. FTIR spectra of the samples in KBr disk were recorded on an E55+FRA106 type IR spectrometer. Raman analysis was performed by a Renishaw inVia Raman microscope using the 514 nm line from an Ar ion laser. The morphology was observed with a Hitachi H2120 transmission electron microscope.

2.3 Electrochemical measurements

Electrochemical experiments were performed in a three-electrode cell using a CHI660A electrochemistry analyzer at room temperature. A platinum coil and an Ag/AgCl were used as a

counter and a reference electrode, respectively. As a working electrode, ND (F-ND, A-ND) powder electrode was prepared as following: A piece of platinum wire (0.1 mm in diameter) was sealed in a small pipette and a small cavity was left at the tip (0.5 mm in diameter). The cavity was filled with ND (F-ND, A-ND) powder by grinding the tip on a glass slide over which the powder was spread. The cyclic voltammograms (CVs) of ND (F-ND, A-ND) powder electrodes in 0.1M KCl electrolytes and the solutions of 0.1M KCl containing 0.05M $K_3[Fe(CN)_6]$ or 0.05M $FeCl_3$ were recorded. The scan rate was set as 0.01-0.2 V/s. The potential amplitude of AC signal was kept as 5 mV and the measured frequency range was 10^{-1} - 10^5 Hz in AC impedance experiments.

3. RESULTS AND DISCUSSION

3.1 Characterizations of F-ND and A-ND

FTIR spectra of untreated ND, F-ND, and A-ND powders are shown in Fig. 1. Most diamond powder products underwent oxidative purification process involving oxidative acid treatment and direct thermal oxidation in air, producing variety of surface oxygen containing groups. The absorption peak of 1733 cm^{-1} was assigned to the modes of stretching C=O vibration in carbonyl groups and the peak observed at 1092 cm^{-1} was C–O vibration in C–O–C groups. The broad absorption band with a peak of $3430\text{--}3450\text{ cm}^{-1}$ and the peak at 1633 cm^{-1} were stretching and deformation C–OH vibrations. Vibrational features appeared at 2922 cm^{-1} and 2850 cm^{-1} corresponded to asymmetric and symmetric stretching C–H vibrations [24]. A peak at 1384 cm^{-1} was due to the OH bending vibration in COOH [24, 25].

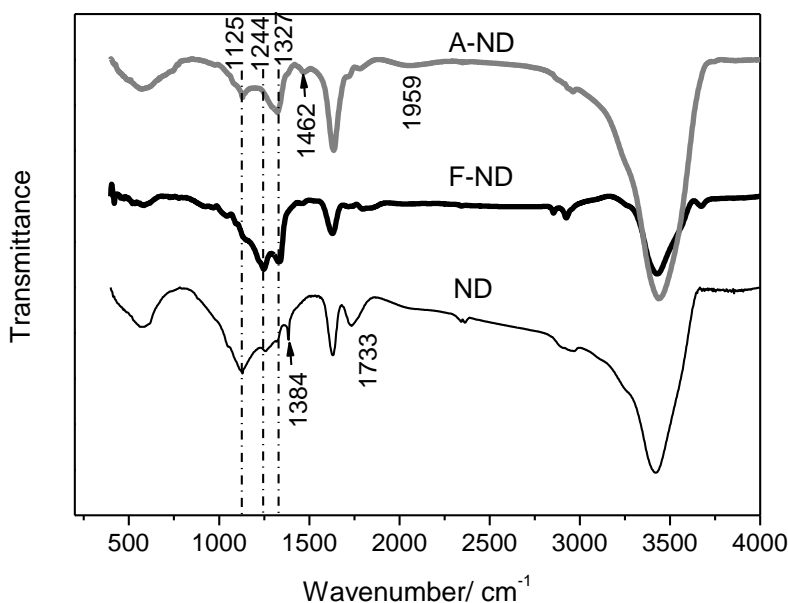


Figure 1. FTIR spectra of ND, F-ND, and A-ND.

The main changes after fluorination treatment were related to the loss of C–O (around 1092 cm^{-1}) and C=O (around 1733 cm^{-1}). The peaks of 1234 cm^{-1} and 1050 cm^{-1} (weak) were attributed to asymmetric and symmetric CF_2 vibrations [9, 26, 27]. The results indicated that fluorine molecules substituted oxygen and chemisorbed onto the diamond surface. Moreover, the peak at 1327 cm^{-1} assigned to the C–C stretching vibrations of the diamond crystal lattice was very weak for untreated ND because it was an inactive mode for infrared spectroscopy. The high electronegativity of fluorine atom induced dipole moments in the C–C bonds. The lack of symmetry in the C–C bonds in the near-surface region resulted in an increase in intensity after fluorination. For A-ND, There is a dramatic increase at the band of $3000\text{--}3600\text{ cm}^{-1}$ and the peak at 1633 cm^{-1} , indicating presence of N–H groups in the A-ND sample. Amines show N–H peaks between $3300\text{--}3450\text{ cm}^{-1}$ (ν_{NH}) and between $1620\text{--}1650\text{ cm}^{-1}$ (δ_{NH}). A wide peak around 1959 cm^{-1} can be attributed to C–NH_3^+ groups [24].

The TEM images obtained for pristine ND powder and F-ND specimen are compared in Fig. 2. It was observed that the aggregate particle size reduced to below 50 nm after fluorination. The pristine ND clusters (Fig. 2A) was drastically deagglomerated by the surface fluorination (Fig. 2B). This also implied that fluorine replaced most functional groups on the ND surface because of its high electronegativity.

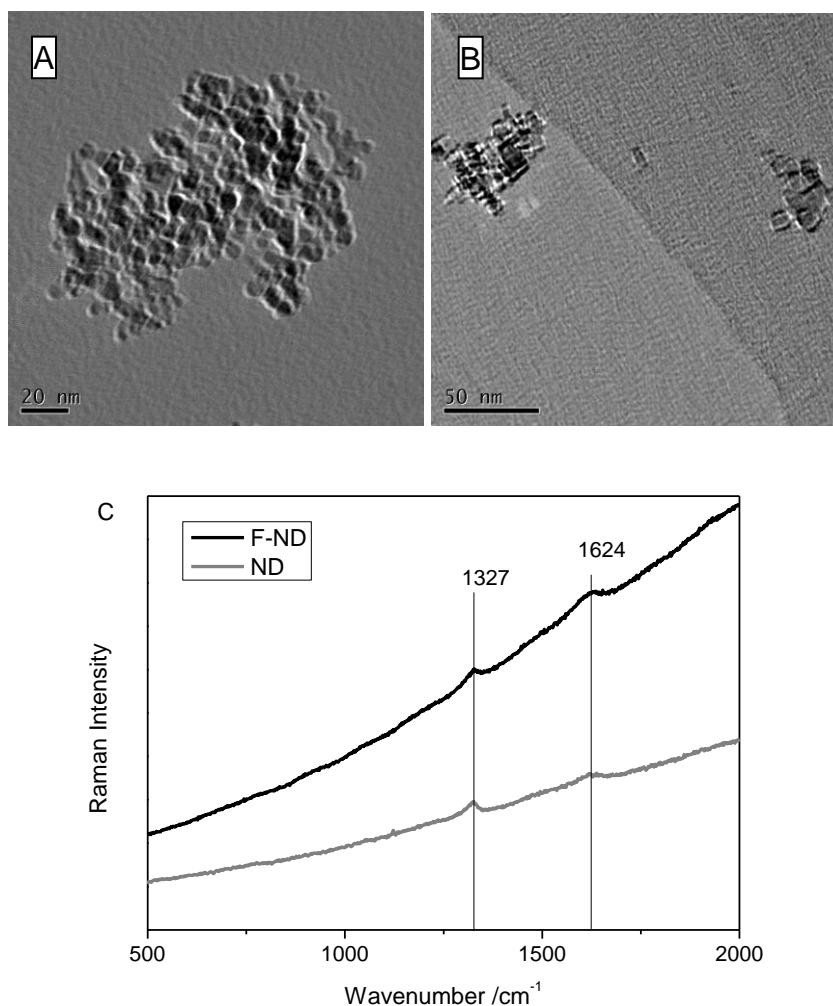


Figure 2. TEM images of ND specimen before (A) and after fluorination at $350\text{ }^\circ\text{C}$ (B), and corresponding Raman spectra (C).

Electrostatic repulsion among the F-ND particles with negative surface charges resulted in the deaggregation of ND powder [28]. The corresponding Raman spectra are shown in Fig. 2C. A peak centered at 1326 cm^{-1} associated with diamond sp^3 bonding scheme. The broadening of the peak and downshifting from the value of 1332 cm^{-1} , which was expected for bulk diamond, was attributed to a phonon confinement effect due to the nanocrystallites' size effects [19]. A small peak around 1620 cm^{-1} was assigned to sp^2 defects on ND's surface [29]. It was clear that the F-ND remained sp^3 bonded diamond crystalline structure after fluorination.

3.2 Electrochemical behavior in $Fe(CN)_6^{3-}/Fe(CN)_6^{4-}$ solution

The electron transfer for $Fe(CN)_6^{3-}/Fe(CN)_6^{4-}$ has been considered to be extremely sensitive to surface properties of the electrodes. Fig. 3 shows the CV curves recorded in $0.1\text{ M KCl} + 0.01\text{ M K}_3[Fe(CN)_6]$ solution at the ND, F-ND, and A-ND powder electrodes, respectively, $\nu=0.02\text{ V/s}$. The separation between the anodic and the cathodic peak (ΔE_p) was 148 mV at the scan rate of 0.02 V/s on the ND electrode, and got larger as the scan rate increased, indicating a quasi-reversible reaction. An increase in ΔE_p (from 148 to 198 mV at 0.02 V/s) and a decrease in peak currents appeared at F-ND electrode showed slower redox kinetics of the $Fe(CN)_6^{3-}/Fe(CN)_6^{4-}$ system. Such behavior can be explained by electrostatic repulsion between the ferri/ferro cyanide redox ions and the dipoles of C–F groups on the F-ND surface [30, 31]. The hydrophobic F-ND surface was also considered to limit the approach of redox probes in the aqueous solution, resulting in a decrease or blocking of redox reactions [14, 32].

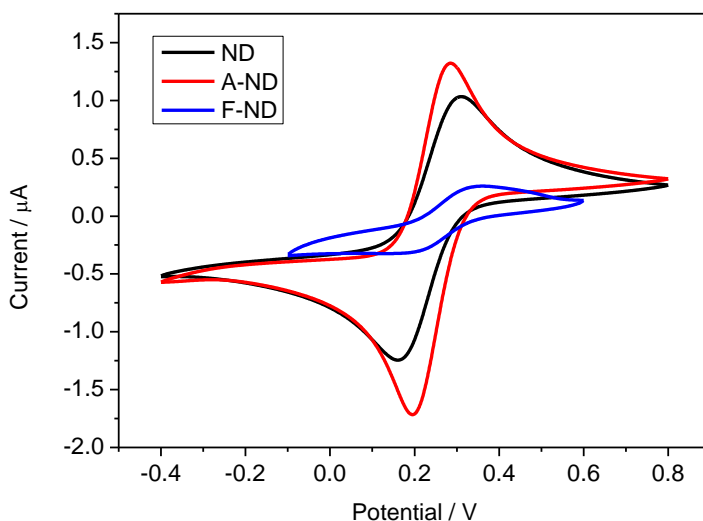


Figure 3. CV curves in $0.1\text{ M KCl}+0.05\text{ M K}_3[Fe(CN)_6]$ solution on ND, F-ND, and A-ND electrodes vs. Ag/AgCl, $\nu = 0.02\text{ V/s}$

The electrochemical behavior of A-ND electrode is rather different to that of the fluorinated surface. The peak separation decreased to 90 mV and both the anodic peak current and cathodic current increased after amino modification. These results suggested that amino-terminated ND surface

can accelerate the electron exchange between the electrode and $\text{Fe}(\text{CN})_6^{3-}/\text{Fe}(\text{CN})_6^{4-}$ in aqueous solution. The increase in the redox reaction rate can be caused by the electrostatic attraction between the positively charged amino groups of the surface and the $\text{Fe}(\text{CN})_6^{3-}/\text{Fe}(\text{CN})_6^{4-}$ anions [33, 34].

Fig. 4A shows Nyquist plots for 0.05 M $\text{K}_3[\text{Fe}(\text{CN})_6]$ in 0.1 M KCl on the electrode surface at the open circuit potential versus Ag/AgCl. The frequency range is $10^{-1}\sim 10^5$ Hz. The magnification of the high-frequency part is shown in Fig. 4B. The impedance plots are characterized by a single semicircle in the high-frequency region, which corresponded to the parallel combination of the charge-transfer resistance R_{ct} and the double layer capacitance C_{dl} , and followed by a low-frequency straight line corresponded to Warburg impedance W . The equivalent circuit is shown in the inset of Fig. 4A. The larger semicircle diameter ($R_{ct}=100$ k Ω) obtained on the F-ND electrode (Fig. 4A), compared to that on the ND electrode ($R_{ct}=3$ k Ω assessed from Fig. 4B), indicated that the fluorination on ND surface enlarged the interfacial resistance, and blocked the electron transfer. While a decrease in the charge-transfer resistance ($R_{ct}=1.2$ k Ω) on the A-ND electrode was observed in Fig. 4B, confirming that the amino modification made the redox reaction on the electrode easier.

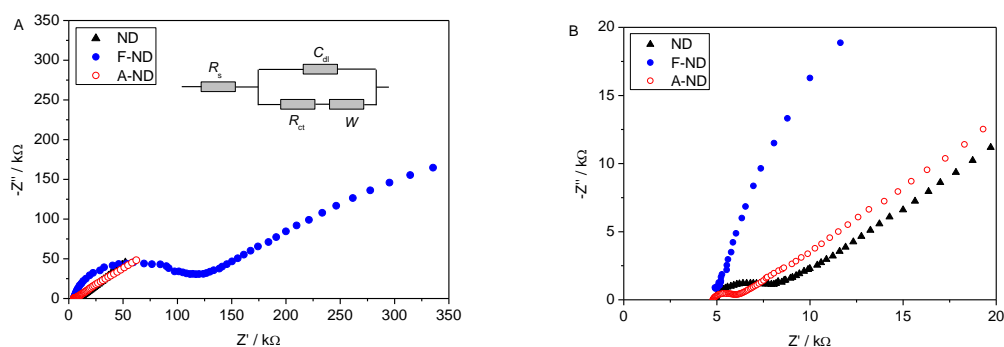


Figure 4. (A) Nyquist plots on the electrode surface in 0.1 M KCl + 0.05 M $\text{K}_3[\text{Fe}(\text{CN})_6]$ solution at the open circuit potential, the inset is the equivalent circuit, (B) Magnification of the high-frequency part.

3.3 Electrochemical behavior in $\text{Fe}^{3+}/\text{Fe}^{2+}$ solution

For the redox couple with cations ($\text{Fe}^{3+}/\text{Fe}^{2+}$), the influences of the surface modifications were different. Fig. 5 shows the CV curves in 0.1 M KCl + 0.05 M FeCl_3 solution on ND, F-ND, and A-ND electrodes, respectively, $\nu=0.02$ V/s. Well-defined anodic and cathodic peaks associated with the oxidation and reduction of the $\text{Fe}^{3+}/\text{Fe}^{2+}$ at the ND/solution interface. The separation ΔE_p was 86 mV at the scan rate of 0.02 V/s, and got larger as the scan rate increased, indicating a quasi-reversible reaction. On the F-ND electrode, lower peak currents and slight bigger ΔE_p showed a high electrochemical inertness of F-ND. The Nyquist plots in Fig. 6B exhibited an enlarged charge-transfer resistance (from 8.9 k Ω for the pristine ND to 35.8 k Ω for F-ND). In general, C–F groups exhibit quite small polarizability, resulting in less interaction with ions and molecules [35, 36]. For the amino-terminated ND surface, a dramatic increase in ΔE_p (as shown in Fig. 5) and R_{ct} (~193 k Ω assessed

from Fig. 6A) showed a more irreversible electrode process because of electrostatic repulsion between the $\text{Fe}^{3+}/\text{Fe}^{2+}$ redox ions and amino groups on the A-ND surface.

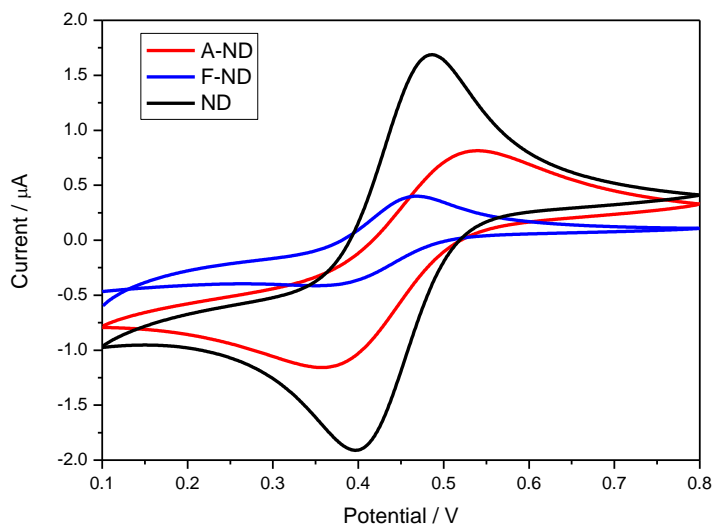


Figure 5. CV curves in 0.1 M KCl + 0.05 M FeCl_3 solution on ND, F-ND, and A-ND electrodes vs. Ag/AgCl, $\nu = 0.02$ V/s.

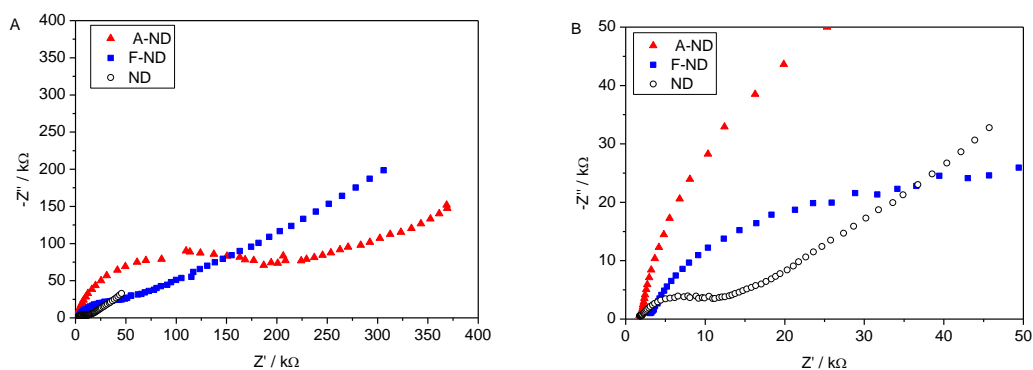


Figure 6. (A) Nyquist plots on the electrode surface in 0.05 M FeCl_3 + 0.1 M KCl solution at the open circuit potential, (B) Magnification of the high-frequency part.

4. CONCLUSIONS

The F-ND was prepared through direct interaction of elemental fluorine with diamond surfaces and A-ND was obtained using F-ND as an intermediate by chemical substitution reactions. The electrochemical results showed that both redox reactions of $\text{Fe}(\text{CN})_6^{3-}/\text{Fe}(\text{CN})_6^{4-}$ and $\text{Fe}^{3+}/\text{Fe}^{2+}$ were quasi-reversible on the pristine ND/solution interfaces. The F-ND surfaces showed slower redox kinetics of the $\text{Fe}(\text{CN})_6^{3-}/\text{Fe}(\text{CN})_6^{4-}$ and $\text{Fe}^{3+}/\text{Fe}^{2+}$ systems. The followed amino modification accelerated the electron exchange between the electrode and $\text{Fe}(\text{CN})_6^{3-}/\text{Fe}(\text{CN})_6^{4-}$ but slowed the redox

reaction of $\text{Fe}^{3+}/\text{Fe}^{2+}$ cations. It suggests that the ND electrochemical probes suitable for different redox reactions can be achieved via surface functionalizations.

ACKNOWLEDGEMENT

This work was supported by National Natural Science Foundation of China (Nos. 50872119 and 50972125), Natural Science Foundation of Hebei Province (Nos. E2010001187 and E2012203112). The authors gratefully acknowledge financial and material support from Element Six Ltd.

References

1. K.B. Holt, *Phil. Trans. R. Soc. A*, 365 (2007) 2845.
2. A. Kruger, *Adv. Mater.*, 20 (2008) 2445.
3. A. Krüger, Y. Liang, G. Jarre, J. Stegk, *J. Mater. Chem.*, 16 (2006) 2322.
4. A. Krueger, *Chemistry-A European Journal*, 14 (2008) 1382.
5. R. Martín, C. Menchón, N. Apostolova, V.M. Victor, M. Álvaro, J.R. Herance, H. García, *ACS Nano*, 4 (2010) 6957.
6. H. Huang, E. Pierstorff, E. Osawa, D. Ho, *Nano Lett.*, 7 (2007) 3305.
7. B. Guan, F. Zou, J. Zhi, *Small*, 6 (2010) 1514.
8. M. Chen, E.D. Pierstorff, R. Lam, S.-Y. Li, H. Huang, E. Osawa, D. Ho, *ACS Nano*, 3 (2009) 2016.
9. Y. Liu, Z. Gu, J.L. Margrave, V.N. Khabashesku, *Chem. Mater.*, 16 (2004) 3924.
10. V. Khabashesku, J. Margrave, E. Barrera, *Diam. Relat. Mater.*, 14 (2005) 859.
11. G. Siné, L. Ouattara, M. Panizza, C. Comninellis, *Electrochem. Solid St.*, 6 (2003) D9.
12. S. Szunerits, C. Jama, Y. Coffinier, B. Marcus, D. Delabouglise, R. Boukherroub, *Electrochem. Commun.*, 8 (2006) 1185.
13. K.-I. Sotowa, T. Amamoto, A. Sobana, K. Kusakabe, T. Imato, *Diam. Relat. Mater.*, 13 (2004) 145.
14. J. Wang, M.A. Firestone, O. Auciello, J.A. Carlisle, *Langmuir*, 20 (2004) 11450.
15. G.J. Zhang, K.S. Song, Y. Nakamura, T. Ueno, T. Funatsu, I. Ohdomari, H. Kawarada, *Langmuir*, 22 (2006) 3728.
16. Y. Coffinier, S. Szunerits, C. Jama, R. Desmet, O. Melnyk, B. Marcus, L. Gengembre, E. Payen, D. Delabouglise, R. Boukherroub, *Langmuir*, 23 (2007) 4494.
17. J.B. Zang, Y.H. Wang, S.Z. Zhao, L.Y. Bian, J. Lu, *Diam. Relat. Mater.*, 16 (2007) 16.
18. L. Chen, J. Zang, Y. Wang, L. Bian, *Electrochim. Acta*, 53 (2008) 3442.
19. K.B. Holt, C. Ziegler, D.J. Caruana, J. Zang, E.J. Millan-Barrios, J. Hu, J.S. Foord, *Phys. Chem. Chem. Phys.*, 10 (2008) 303.
20. K.B. Holt, C. Ziegler, J. Zang, J. Hu, J.S. Foord, *J. Phys. Chem. C*, 113 (2009) 2761.
21. K.B. Holt, D.J. Caruana, E.J. Millan-Barrios, *J. Am. Chem. Soc.*, 131 (2009) 11272.
22. W. Zhao, J.J. Xu, Q.Q. Qiu, H.Y. Chen, *Biosens. Bioelectron.*, 22 (2006) 649.
23. J. Zang, Y. Wang, L. Bian, J. Zhang, F. Meng, Y. Zhao, S. Ren, X. Qu, *Electrochim. Acta*, 72 (2012) 68.
24. S. Hens, G. Cunningham, T. Tyler, S. Moseenkov, V. Kuznetsov, O. Shenderova, *Diam. Relat. Mater.*, 17 (2008) 1858.
25. O.A. Williams, J. Hees, C. Dieker, W. Jäger, L. Kirste, C.E. Nebel, *ACS Nano*, 4 (2010) 4824.
26. M. Ray, O. Shenderova, W. Hook, A. Martin, V. Grishko, T. Tyler, G. Cunningham, G. McGuire, *Diam. Relat. Mater.*, 15 (2006) 1809.
27. T. Ando, K. Yamamoto, M. Matsuzawa, Y. Takamatsu, S. Kawasaki, F. Okino, H. Touhara, M. Kamo, Y. Sato, *Diam. Relat. Mater.*, 5 (1996) 1021.
28. H. Huang, Y.H. Wang, J.B. Zang, L.Y. Bian, *Appl. Surf. Sci.*, 258 (2012) 4079.

29. S. Praver, K. Nugent, D. Jamieson, J. Orwa, L.A. Bursill, J. Peng, *Chem. Phys. Lett.*, 332 (2000) 93.
30. B. Guan, J. Zhi, X. Zhang, T. Murakami, A. Fujishima, *Electrochem. Commun.*, 9 (2007) 2817.
31. M. Miyamoto, Y. Tanaka, M. Furuta, T. Kondo, A. Fujishima, K. Honda, *Electrochim. Acta*, 54 (2009) 3285.
32. H. Uetsuka, D. Shin, N. Tokuda, K. Saeki, C.E. Nebel, *Langmuir*, 23 (2007) 3466.
33. P. Actis, A. Denoyelle, R. Boukherroub, S. Szunerits, *Electrochem. Commun.*, 10 (2008) 402.
34. V.N. Mochalin, I. Neitzel, B.J.M. Etzold, A. Peterson, G. Palmese, Y. Gogotsi, *ACS Nano*, 5 (2011) 7494.
35. T. Kondo, *Diam. Relat. Mater.*, 17 (2008) 48.
36. T. Kondo, H. Ito, K. Kusakabe, K. Ohkawa, Y. Einaga, A. Fujishima, T. Kawai, *Electrochim. Acta*, 52 (2007) 3841.